Thermodynamic stability and diffusivity of near-equiatomic Ni–Mn alloys

Ling Ding, Peter F. Ladwig, Xinyan Yan, and Y. Austin Chang[a)]
Department of Materials Science and Engineering, University of Wisconsin, Madison, Wisconsin 53706

(Received 29 October 2001; accepted for publication 11 December 2001)

The equilibrium phase diagram of the nickel-manganese system is determined between 500 and 850 °C, in the composition range between 25 and 70 at. % Ni. A combination of electron probe microanalysis, x-ray diffraction, and optical microscopy was employed to analyze 47 samples that were annealed anywhere from three to seven months. The equiatomic, antiferromagnetic, $L1_0$-NiMn phase that is of considerable technological interest was found to exist continuously between 500 and 700 °C. No other intermediate phases were found in this study at low temperatures. These results are in contrast to the currently accepted phase diagram published in most handbooks. A hot-isobaric-pressing method was used to initially bond samples that were subsequently used to determine interdiffusion coefficients in the Ni–Mn system at 650 °C. The Boltzmann–Matano method [T. Heumann, Z. Phys. Chem. **201**, 168 (1952)] allowed the calculation of these interdiffusion coefficients across the α-Mn, β-Mn, γ-Mn, $L1_0$-NiMn, and γ-Ni phases. © *2002 American Institute of Physics.* [DOI: 10.1063/1.1450042]

Equiatomic Ni–Mn thin films are of interest to the magnetic storage industry for use in magnetoresistive sensors.[1] In these sensors, exchange coupling between an antiferromagnetic film, such as NiMn, and a soft ferromagnetic film is required to hold or ''pin'' the magnetization within the ferromagnetic layer.[1] However, the $L1_0$ phase of NiMn is the only antiferromagnetic phase of this intermetallic, and is thus the only phase suitable for use in these sensors. Therefore, understanding the compositional and temperature ranges over which this antiferromagnetic phase is stable is extremely important but is made very difficult due to the vast inconsistencies between published equilibrium phase diagrams. Furthermore, there is no existing diffusion coefficient information for Ni–Mn alloys in the equiatomic range. Diffusion coefficient information is of significant importance because interlayer diffusion is a primary long-term failure mechanism in magnetoresistive sensors. In the present study, we apply information gained from experiments to resolve the controversy between existing phase diagrams as well as report reliable diffusion coefficients for NiMn alloys.

NiMn exists in three solid polymorphic phases at the equiatomic concentration: a high-temperature (*H*), chemically disordered, face-centered-cubic (fcc) *A*1 phase; a midtemperature (*M*), chemically ordered, cubic *B*2 phase; and a low-temperature (*L*), antiferromagnetic, chemically ordered, tetragonal $L1_0$ phase.[2] The $L1_0$ structure is simple tetragonal with a two atom basis that resembles a non-Bravais, body/face-centered-tetragonal structure. Although all previously published phase diagrams report the existence of these three phases, their reported equilibria are drastically different. For example, the phase diagram as determined by Coles and Hume-Rothery[3] shows a $L1_0$ phase that is stable from room temperature to 700 °C, while Tsiuplakis and Kneller[4] reported a much more complicated phase diagram which claims that no single phase is stable at the equiatomic composition between 480 and 620 °C. The controversies extend much further beyond this, with some diagrams showing the presence of as many as five different solid phases present at various temperatures in the equiatomic region.[4]

The alloys for both phase diagram determination and interdiffusion coefficient measurements were prepared by arc melting 99.98% pure Ni slugs and 99.99% pure Mn chips, in a 99.998% pure Ar atmosphere. Each piece of raw material was etched, rinsed, and dried to remove all surface oxidation. The completely mixed alloys were cast into rods and sliced into disks for use in subsequent experiments. Unless otherwise mentioned, all samples were sealed in evacuated quartz tubes before annealing in resistive-element-type tube furnaces.

For phase diagram determination, alloys were first homogenized at high temperature (950 °C for 72 h) before being transferred to a furnace at the desired long-term annealing temperature in which the phase equilibrium was reached. In this study, the annealing time is 7 months for samples annealed at temperatures below 700 °C, and at least 3 months for samples annealed at 700 °C and above. After annealing, alloys were first examined via optical microscopy (Olympus with SPOT software) and then examined by electron microprobe analysis [(EMPA), Camerca SX-50] for phase composition identification. X-ray diffraction [(XRD), Phillips PW1729, Cu $K\alpha$ radiation] was used for structure identification.

Seven samples were used to determine the phase equilibria in the *B*2-NiMn(*M*) phase region. During quenching, the *B*2-NiMn(*M*) phase transformed, leaving a characteristic martensitic structure, while the face-centered-cubic phase, γ-Mn,Ni, was featureless by comparison. Using EMPA, the phase boundaries of the *B*2 phase were confidently determined and are shown in Fig. 1. The presently determined phase boundaries are in reasonable agreement with those determined from microscopical methods by Coles[3,5] and by differential thermal analysis methods by Tsiuplakis.[4] When compared with the phase diagram as determined by Coles, the *B*2 single phase field shifts about 1 at. % to the Mn-rich

a)Electronic mail: chang@engr.wisc.edu

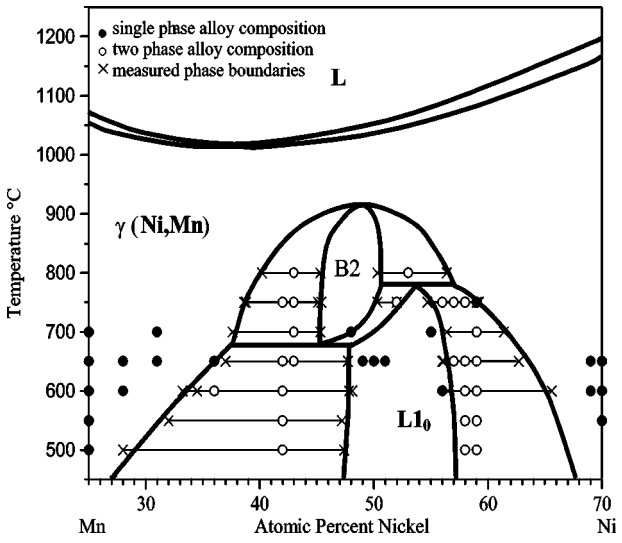

FIG. 1. Experimentally determined, partial NiMn phase diagram. Alloy compositions and resulting phase boundaries are labeled.

side, the γ-Mn/(γ-Mn+$B2$) phase boundary shifts to the Mn-rich side about 2 at. % and the γ-Ni/(γ-Ni+$B2$) phase boundary remains unchanged. The two invariant temperatures of the peritectoid and eutectoid reactions involving the $B2$ phase are close to previously reported values.

The phase boundaries involving the $L1_0$-NiMn(L) phase were examined carefully with more than 20 samples in this study. These results are also shown in Fig. 1. The sizes of each phase region in the samples annealed at 650 °C and above are nominally larger than 3–5 μm, which is sufficiently large for accurate EMPA analysis. As the annealing temperature is decreased to 600 °C, the grain size of the $L1_0$ phase decreases, but phase boundaries can still be determined by careful EMPA analysis. However, determination of the phase boundaries involving the $L1_0$ phase at 550 and 500 °C was found to be very difficult.

Figure 2 shows the microstructure of a sample with 42 at. % Ni annealed at 500 °C for 220 days. Under a microscope one can see the grains clearly, with the accumulation

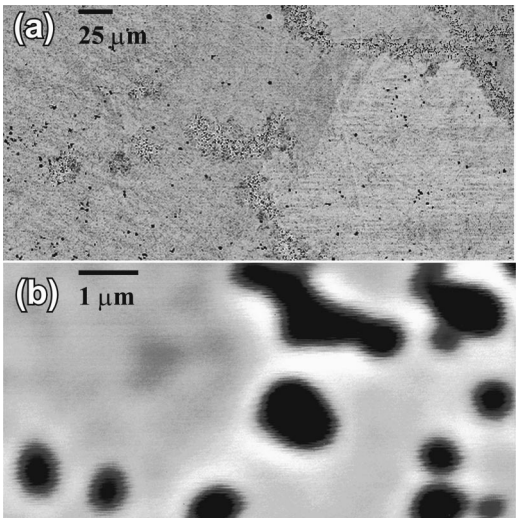

FIG. 2. Microstructure of a 42 at. % Ni sample annealed at 500 °C for 220 days: (a) unetched, low-magnification optical image and (b) high-magnification, BSE image showing compositional variations surrounding pores.

of voids at the boundaries [Fig. 2(a)]. However, no second phase can be observed by optical examination. In backscattered electron (BSE) images of the sample [Fig. 2(b)] we can see the voids with lightly shaded regions surrounding them. However, since these light colored areas are very small in size (less than 1 μm wide), it is almost impossible to position the electron beam for composition determination with the precision necessary using typical EMPA techniques. In this case of very fine microstructure, precise positioning and acquisition are needed at scales finer than the stage mechanism is capable of producing. To achieve this precision, a beam deflection technique was used, in which the position of the beam is moved using magnetic fields rather than moving the sample stage. Using this technique, the $L1_0/\gamma$-Mn phase boundaries were successfully measured and are shown in Fig. 1.

The sizes of the $L1_0$ and γ-Ni phases in Ni-rich samples are normally much smaller than the $L1_0$ and γ-Mn phases in Mn-rich samples annealed at the same temperature. Therefore, in the four Ni-rich samples annealed at 500 and 550 °C, no precipitate phases were found even with high-magnification backscattered images. X-ray powder diffraction analysis was performed on one such sample (59 at. % Ni, 500 °C), and only the $L1_0$-NiMn(L) phase was detected. It is noteworthy that, in our judgment, the equilibrium state may not have been reached in these four samples even after 220 days of annealing. Since very small amounts of a second phase may not be detected by XRD or EMPA, more work needs to be done in this region using other techniques.

Hot-isobaric pressing (HIP) was used to form diffusion multiples in the present study. A Ni|Mn|$Ni_{50}Mn_{50}$|$Ni_{56}Mn_{44}$ diffusion multiple was made by placing four 4-mm-thick alloy disks (one of each composition) inside a pure Ni cylinder. These four alloys were previously homogenized and the size of the disks was designed such that the dimensions were significantly larger than diffusion distances. After electron-beam welding Ni end members to the cylinder, the diffusion multiple underwent a HIP run of 4 h at 950 °C under a 200 MPa (2000 atm) pressure to provide good contact between components. Following the HIP, the diffusion multiple was sealed in an evacuated quartz tube for further diffusion heat treatment. Diffusion annealing was performed at 650 °C for two months. Concentration profiles across the diffusion zones were measured by electron microprobe. NiMn alloys with a uniform composition of 50 at. % Ni were selected as calibration standards. After diffusion heat treatment, the diffusion multiple was mounted in epoxy, sectioned perpendicular to the interfaces, and polished. The composition profiles were determined via an EMPA line scan perpendicular to the interface. The line scan step that was used varied between 1 and 5 μm, depending on the width of the diffusion layers. Figure 3 shows the concentration profile obtained across the Ni|Mn interface within a diffusion multiple. Concentration profiles across other interfaces were also obtained. It is noteworthy that the concentrations at the phase boundaries within the diffusion zones are comparable to those found in the phase diagram analysis. As we can see from Fig. 3, intermetallic phases and solid solutions of Ni–Mn formed in the diffusion zone.

The Boltzmann–Matano method was used to compute

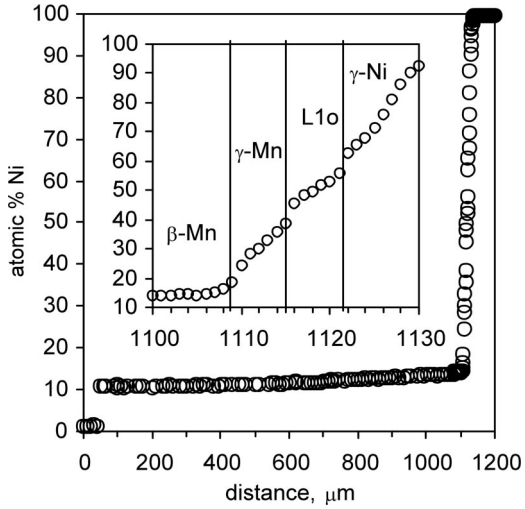

FIG. 3. Concentration profile across the Ni|Mn interface in a diffusion multiple annealed at 650 °C. Inset is an enlargement of the high slope region.

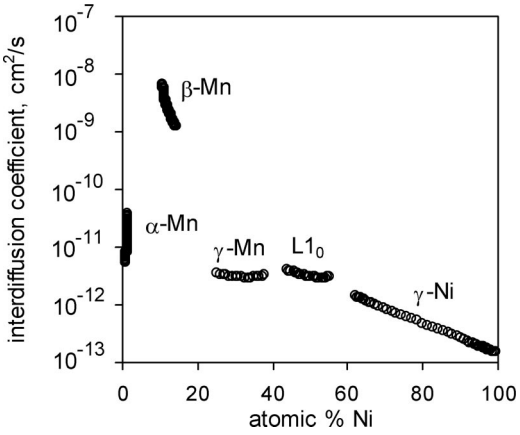

FIG. 4. Calculated interdiffusion coefficients, $\tilde{D}$, at 650 °C.

the interdiffusion coefficients in such a multiphase system.[6] Calculated interdiffusion coefficients, $\tilde{D}$, at 650 °C in different phases are shown in Fig. 4. It is interesting to note that $\tilde{D}$ in the β-Mn phase (10^{-8} cm^2/s) is 3–4 orders larger than diffusion coefficients in the other phases, due to its relatively open bcc structure. The interdiffusion coefficient in the $L1_0$ phase was also calculated from a concentration profile measured across the $Ni_{50}Mn_{50}|Ni_{56}Mn_{44}$ interface. The results from the multiphase system of the Ni|Mn diffusion couple are quite similar to those from the single-phase, $Ni_{50}Mn_{50}|Ni_{56}Mn_{44}$ diffusion couple.

The equilibrium phase diagram of the Ni–Mn system in the composition range between 25 and 70 at. % Ni was determined using EMPA with the aid of optical microscopy and x-ray diffraction. It was found that the $L1_0$-NiMn(L) phase exists at temperatures up to 750 °C. Intermediate phases $NiMn_2$ and Ni_2Mn reported by Tiuplakis[4] were not found in this study. These results are more complimentary to the original work performed by Coles and Hume-Rothery,[3] and are in stark contrast to the generally accepted Ni–Mn phase diagrams in most current handbooks.[7] We are convinced that these diagrams do not reflect equilibrium conditions.

The HIP bonding method was used to create diffusion multiples in which interdiffusion coefficients could be measured at relatively low temperatures. Interdiffusion coefficients of the technologically important $L1_0$ phase were calculated at 650 °C from single-phase and multiphase diffusion couples with good agreement. Interdiffusion coefficients for all equilibrium phases at 650 °C were determined as well.

The authors wish to thank the Division of Materials Sciences, Office of Basic Energy Research of DOE for financial support through Grant No. DE-FG02-99ER45777.

[1] T. Lin, D. Mauri, N. Staud, C. Hwang, J. K. Steward, and G. L. Gorman, Appl. Phys. Lett. **65**, 1183 (1994).
[2] K. Adachi and C. M. Wayman, Metall. Trans. A **16**, 1567 (1985).
[3] B. R. Coles and W. Hume-Rothery, J. Inst. Met. **80**, 85 (1951).
[4] V. K. E. Tsiuplakis and E. Kneller, Z. Metallkd. **60**, 443 (1969).
[5] B. R. Coles, J. Phase Equilib. **16**, 108 (1995).
[6] T. Heumann, Z. Phys. Chem. (Leipzig) **201**, 168 (1952).
[7] *Binary Alloy Phase Diagrams*, 2nd ed., edited by T. B. Malssaski, J. L. Murray, L. H. Bennett, and H. Baker (ASM, Materials Park, OH, 1986).